Cerebral Cortex November 2015;25:4135–4145
doi:10.1093/cercor/bhu133
Advance Access publication June 16, 2014

Correspondence Between Aberrant Intrinsic Network Connectivity and Gray-Matter Volume in the Ventral Brain of Preterm Born Adults

Josef G. Bäuml[1,3,†], Marcel Daamen[4,5,†], Chun Meng[1,3], Julia Neitzel[1,3], Lukas Scheef[4], Julia Jaekel[6,8], Barbara Busch[5], Nicole Baumann[6], Peter Bartmann[5], Dieter Wolke[6,7], Henning Boecker[4], Afra M. Wohlschläger[1,3] and Christian Sorg[1,2,3]

[1]Department of Neuroradiology,, [2]Department of Psychiatry, Klinikum rechts der Isar and, [3]TUM-NIC Neuroimaging Center, Technische Universität München, München, Germany, [4]Functional Neuroimaging Group, Department of Radiology and, [5]Department of Neonatology, University Hospital Bonn, Bonn, Germany, [6]Department of Psychology and, [7]Warwick Medical School, University of Warwick, Coventry, UK and [8]Department of Developmental Psychology, Ruhr-University Bochum, Bochum, Germany

[†]Josef G. Bäuml and Marcel Daamen contributed equally to this study.

Address correspondence to Dr Christian Sorg, Department of Psychiatry and Neuroradiology, Klinikum rechts der Isar, Ismaninger Strasse 22, 81675 Munich, Germany. Email: c.sorg@lrz.tu-muenchen.de

Widespread brain changes are present in preterm born infants, adolescents, and even adults. While neurobiological models of prematurity facilitate powerful explanations for the adverse effects of preterm birth on the developing brain at microscale, convincing linking principles at large-scale level to explain the widespread nature of brain changes are still missing. We investigated effects of preterm birth on the brain's large-scale intrinsic networks and their relation to brain structure in preterm born adults. In 95 preterm and 83 full-term born adults, structural and functional magnetic resonance imaging at-rest was used to analyze both voxel-based morphometry and spatial patterns of functional connectivity in ongoing blood oxygenation level–dependent activity. Differences in intrinsic functional connectivity (iFC) were found in cortical and subcortical networks. Structural differences were located in subcortical, temporal, and cingulate areas. Critically, for preterm born adults, iFC-network differences were overlapping and correlating with aberrant regional gray-matter (GM) volume specifically in subcortical and temporal areas. Overlapping changes were predicted by prematurity and in particular by neonatal medical complications. These results provide evidence that preterm birth has long-lasting effects on functional connectivity of intrinsic networks, and these changes are specifically related to structural alterations in ventral brain GM.

Keywords: brain structure, intrinsic network, preterm birth, preterm born adults, structure–function relationship

Introduction

The human brain is highly susceptible to the consequences of preterm birth owing to the higher risk of peri- and neonatal brain injury (Deng 2010). Neurobiological models of early brain injury propose that primary destructive processes (e.g., loss of oligodendrocytes due to hypoxic or ischemic events) are followed by secondary maturational disturbances (Pierson et al. 2007; Volpe 2009) and provide valid explanations for the adverse impact of preterm birth at microscale (Selip et al. 2012; Salmaso et al. 2014). However, our systematic understanding of the consequences of preterm birth on the large-scale brain level is limited. Functional (fMRI) and structural (sMRI) magnetic resonance imaging studies have demonstrated widely distributed effects of preterm birth on newborns' (Fransson et al. 2007; Smyser et al. 2010), children (Zubiaurre-Elorza et al. 2011; Griffiths et al. 2013), and even young adults' brains (Nosarti et al. 2008, 2009; Myers et al. 2010; Eikenes et al. 2011; Mullen et al. 2011). Yet, both the spatial pattern of functional and structural changes and their possible relationship among each other are poorly understood. To address this issue, the present study investigated the long-term effects of preterm birth on the plethora of the brain's intrinsic large-scale networks and relates potential changes with structural brain alterations in preterm born adults.

Intrinsic networks represent a basic form of functional large-scale brain organization (Biswal et al. 1995; Vincent et al. 2007; Bressler and Menon 2010; Sepulcre et al. 2010). They are characterized by spatially and temporally coherent fluctuations in the low-frequency range (<0.1 Hz) of the blood oxygenation level–dependent (BOLD) signal measured by resting-state fMRI. They correspond to known neuroanatomical systems and are consistent across individuals (Damoiseaux et al. 2006), different states of consciousness (Horovitz et al. 2008), development (Fransson et al. 2007), and even species (Vincent et al. 2007). Precursors of intrinsic brain networks (IBNs) are already detectable in newborns (Fransson et al. 2009) and even preterm born infants (Doria et al. 2010), with the latter showing subtle alterations in network connectivity (Damaraju et al. 2010; Smyser et al. 2010). Although the influence of preterm birth on functional networks has been demonstrated in the short term, little is known about the long-term consequences and whether these reach into adulthood. In particular, it is unknown how the long-term effects of preterm birth manifest in the whole range of IBNs.

Preterm born individuals have been repeatedly shown to have regional structural alterations that persist into adulthood. Recent studies of preterm born adolescents and young adults using voxel-based morphometry (VBM) suggest that both white and gray-matter (GM) alterations are found (Nosarti et al. 2008; Spencer et al. 2008). Considering that IBNs are a basic large-scale organizational principle of the primate brain, we speculated that putative GM anomalies would also be associated with functional connectivity changes of corresponding intrinsic networks.

To investigate intrinsic networks and their relationship with structural changes, we performed spatial independent component analysis (ICA) on resting-state fMRI (rs-fMRI) data (Sorg et al. 2007, 2013) and VBM on structural MRI data in 95 preterm and 83 full-term born adults. Spatial ICA decomposes rs-fMRI data into components reflecting intrinsic networks (Fox and Raichle 2007). ICA is a model-free multivariate data

analysis approach that—assuming linear mixtures of independent sources—decomposes data into temporally coherent spatial components by estimating maximally independent spatial sources (Beckmann et al. 2005). VBM on structural MRI data encompasses a voxel-wise comparison of the local concentration of brain tissue between groups of subjects (Ashburner and Friston 2000) and has proven to be a useful tool to investigate the long-term effect of preterm birth on brain structure (Nosarti et al. 2008). We hypothesized that adults born preterm show 1) widespread alterations in the functional connectivity of IBNs, 2) widespread structural GM changes, and 3) that structural and functional changes would be specifically associated. 4) Finally, we assumed that, in regions of correspondent changes, alterations in both brain structure and connectivity are predicted by degree of prematurity or associated neonatal medical complications.

Materials and Methods

Participants

Participants were recruited as part of the prospective Bavarian Longitudinal Study (BLS) (Riegel et al. 1995; Wolke and Meyer 1999). The BLS investigates a geographically defined whole-population sample of neonatal at-risk children and healthy term controls. All live-birth infants that were born between February 1985 and March 1986 in southern Bavaria and who required admission to 1 of 19 neonatal units in 17 children's hospitals within the first 10 days of life comprised the target sample (Wolke and Meyer 1999). A total of 7505 children (10.6% of all live births) were classified as neonatal at-risk children, whereupon 2759 children were born before 37 weeks of gestation (Riegel et al. 1995). During the same period, 916 term healthy infants (>36 weeks gestation; normal postnatal care) born in the same hospital centers were recruited as control infants. Over the years, subjects of both groups were repeatedly assessed with neurological and psychological test batteries, and parental interviews to monitor development. Full details of the sampling criteria and dropout rates are provided elsewhere (Wolke and Meyer 1999; Gutbrod et al. 2000). At the age of 26 and based on previous follow-up participation, 435 of preterm born children were willing to participate a follow-up assessment. From the control group, 350 survivors were selected to be similar regarding the overall distribution of child gender, family socioeconomic status (SES), and maternal age of the preterm group. Of this sample, 96 preterm subjects (born before 37 week of gestation) and 84 full-term adult subjects (aged 25–27 years) agreed to undergo functional and structural MRI. MRI assessments were carried out at 2 different sites: the Department of Neuroradiology, Klinikum Rechts der Isar, Technische Universität München, Germany ($N = 113$), and the Department of Radiology, University Hospital Bonn, Germany ($N = 67$). The study was approved by the local ethics committees of the Klinikum rechts der Isar and University Hospital Bonn. All study participants gave written informed consent and received travel expenses and a payment for attendance.

Birth-Related Variables

Gestational age (GA) was estimated from maternal reports of the last menstrual period and serial ultrasounds during pregnancy. In cases where the 2 measures differed by more than 2 weeks, clinical assessment with the Dubowitz method was applied (Dubowitz et al. 1970). Maternal age and birth weight (BW) was obtained from obstetric records. Neonatal medical complications were assessed with a standardized optimality scoring system (Opti) including 21 items (e.g., ventilation or intubation, sepsis, neonatal seizures, cerebral hemorrhage) (Prechtl 1967). Items were coded as 1 (nonoptimal) or 0 (optimal) with the higher value being less optimal. Additionally, the duration of hospitalization until discharge from hospital was recorded from neonatal records. In the following, GA, BW, and Opti are all subsumed under the umbrella term prematurity measures.

Family Socioeconomic Background

The SES was collected through structured parental interviews within 10 days of child birth. It was computed as a weighted composite score based on the profession of the self-identified head of each family together with the highest educational qualification held by either parent (Bauer 1988).

Cognitive Assessment

Prior to and independent from the subsequent MRI examination, subjects from the BLS cohort were asked to take part in an assessment of global cognitive functioning at the age of 26 years by trained psychologists. This included a short version of the German version of the Wechsler Adult Intelligence scale-III (WAIS-III) (Von Aster et al. 2006) allowing of the computation of Full-Scale IQ, Verbal IQ, and Performance IQ. Cognitive and biological data were analyzed using IBM SPSS 20 (IBM Corp., Armonk, NY, USA).

MRI Data Acquisition

At both sites, MRI data acquisition was initially performed on Philips Achieva 3T TX systems (Achieva, Philips, the Netherlands), using an 8-channel SENSE head coil. Due to a scanner upgrade, data acquisition in Bonn had to switch to Philips Ingenia 3T system with an 8-channel SENSE head coil after $N = 17$ participants. To account for possible confounds introduced by scanner differences, functional and structural data analyses included scanner identities as covariates of no interest. Across all scanners, sequence parameters were kept identical. Scanners were checked regularly to provide optimal scanning conditions. Signal-to-noise ratio (SNR) was not significantly different between scanners (one-way ANOVA with factor "scanner-ID" [Bonn 1, Bonn 2, Munich]; $P = 0.811$). Resting-state data were collected for 10 min 52 s from a gradient-echo echo-planar sequence (TE = 35 ms, TR = 2608 ms, flip angle = 90°, FOV = 230 mm^2, matrix size = 64 × 63, 41 slices, thickness 3.58 and 0 mm interslice gap, reconstructed voxel size = 3.59 × 3.59 × 3.59 mm^3) resulting in 250 volumes of BOLD fMRI data per subject. Subsequently, a high-resolution T_1-weighted 3D-MPRAGE sequence (TI = 1300 ms, TR = 7.7 ms, TE = 3.9 ms, flip angle = 15°; 180 sagittal slices, FOV = 256 × 256 × 180 mm, reconstruction matrix = 256 × 256; reconstructed voxel size = 1 × 1 × 1 mm^3) was acquired. Immediately before undergoing the resting-state sequence, subjects were instructed to keep their eyes closed and to restrain from falling asleep. We verified that subjects stayed awake by interrogating via intercom immediately after the rs-fMRI scan. One participant fell asleep and had to be excluded from further analysis.

Analysis of fMRI Data

Data Preprocessing

Functional fMRI data were preprocessed according to an automated in-house pipeline (Meng et al. 2013) using SPM8 (Wellcome Trust Centre for Neuroimaging, University College London, UK: http://www.fil.ion.ucl.ac.uk/spm [date last accessed 3 June 2014]). For each participant, the first 5 functional scans of each resting-state fMRI session were discarded due to magnetization effects. Resulting volumes were then realigned to correct for head motion and co-registered to the structural T_1 image. Subsequently, the T_1-weighted image was segmented into its different compartments using Unified Segmentation (Ashburner and Friston 2005). To transform the individual images into common Montreal Neurological Institute (MNI) space, segmentation-based normalization parameters were applied to the co-registered structural and functional data. Furthermore, normalized EPI images were smoothed using a Gaussian kernel with a full-width at half-maximum (FWHM) of 6 mm to increase SNR. In a final step, preprocessed functional time-series for each voxel were despiked using ANFI's 3dDespike motion censoring procedure (http://afni.nimh.nih.gov/afni [date last accessed 3 June 2014]) to further remove motion-induced artifacts. One subject had to be excluded due to severe image artifacts. Excessive head motion (cumulative motion translation or rotation >5 mm or 3° and mean point-to-point translation or rotation >0.15 mm or 0.1°) was applied as exclusion criterion. To ensure data quality, particularly concerning motion-induced artifacts, temporal SNR (tSNR) and point-to-point head motion were estimated for each subject

(Murphy et al. 2007; Van Dijk et al. 2012). Point-to-point motion was defined as the absolute displacement of each brain volume compared to its previous volume. Two-sample *t*-tests yielded no significant differences between groups regarding mean point-to-point translation or rotation of any direction ($P = 0.12$) as well as tSNR ($P = 0.28$).

Group-Independent Component Analysis

Preprocessed data from both groups was entered into a single group ICA framework as implemented in the GIFT toolbox (GIFT v1.3 h; http://icatb.sourceforge.net [date last accessed 3 June 2014]). We chose a high model order ICA (number of independent components [ICs] = 75 (Allen et al. 2011)) since it has been shown that such models decompose data into components that are in best agreement with known anatomical and functional networks (Kiviniemi et al. 2009). Before performing ICA, a two-step data-reduction approach was conducted using principal component analysis (PCA). First, PCA was done on the single subject level retaining 100 principal components. Large numbers of subject-specific principal components preserve most of the individual variance and have been shown to stabilize subsequent back-reconstruction (Erhardt et al. 2011). In a second step, each of the subject's reduced data was concatenated in time to perform a second PCA on the group level followed by ICA with the infomax algorithm. ICs were depicted as spatial maps and corresponding IC time courses. To estimate the reliability of the decomposition, ICA was repeated 20 times by using the Icasso-toolbox (http://research.ics.aalto.fi/ica/icasso/ [date last accessed 3 June 2014]). Reliability was quantified using the Icasso cluster quality index IQ, ranging from 0 to 1. The group ICA framework in GIFT results in a set of average group components, which are then back reconstructed into single subject space using the GICA3 back-reconstruction method. Each back-reconstructed component consists of a spatial *z*-map reflecting component's functional connectivity pattern across space and an associated time course reflecting component's activity across time. Spatial *z*-maps were used as surrogates of networks' intrinsic functional connectivity (iFC) and analyzed further.

Selection of Intrinsic Brain Networks

To automatically select independent components reflecting intrinsic networks, we conducted multiple spatial regressions on 75 independent components' spatial maps using T-maps of 28 intrinsic connectivity networks as described in Allen et al. (2011). These T-maps (Fig. 4 in Allen et al. (2011)) were based on 603 healthy adolescents and adults and were made available online by the Medical Image Analysis Lab (MIALAB) (http://mialab.mrn.org/data/hcp/RSN_HC_unthresholded_tmaps.nii [date last accessed 3 June 2014]). For each network, the independent component with the largest correlation coefficient was chosen. Beyond Allen's templates, visual inspection by 2 independent raters revealed 4 further components. We identified 2 additional subcortical networks, one covering the thalamus (Thal in Fig. 1) and one covering the medio-temporal lobes including the hippocampus (HC in Fig. 1). Furthermore, we found a bilateral central executive network (bilatCE) and a subnetwork of the salience network (Sal II). Since all of these networks fulfilled the criteria of stability (ICASSO >0.95) and were located in GM, we included them into further analysis.

Statistical Analysis of Group Differences

To statistically evaluate spatial maps of selected independent components, we calculated voxel-wise one-sample *t*-tests on participants' reconstructed spatial *z*-maps for all subjects, using SPM 8 ($P < 0.001$, uncorrected). For group comparisons, these one-sample *t*-test masks were then used to restrict the search space in the subsequent two-sample *t*-test. The two-sample *t*-tests for *z*-maps were controlled for the effect of gender and scanner identity. Resulting maps were thresholded at a family-wise error (FWE) cluster-corrected value of $P < 0.05$. Only significant clusters, containing >20 voxels, are reported here.

Analysis of Structural MRI data

As described recently (Sorg et al. 2013), we used the VBM8 toolbox (http://dbm.neuro.uni-jena.de/vbm.html [date last accessed 3 June 2014]) to analyze brain structure via VBM T_1-weighted images were corrected for bias-field inhomogeneity, registered using linear (12-parameter affine) and nonlinear transformations, and tissue-classified into GM, white matter, and cerebrospinal fluid within the same generative model. The resulting GM images were modulated to account for structural changes resulting from the normalization process. Here, we only considered nonlinear changes so that further analyses did not have to account for differences in head size. Finally, images were smoothed with a Gaussian kernel of 8 mm (FWHM). For group comparisons, voxel-wise two-sample *t*-tests were performed ($P < 0.05$ FWE-corrected, cluster extent 20) controlling for gender and scanner identity.

Analysis of the Relationship Between Functional Connectivity, Structural Morphometry, and Measures of Preterm Birth

iFC–VBM relationship

To analyze the relationship between iFC and brain structure in preterm born adults, we performed both voxel-wise and region-of-interest-based (ROI) approaches. 1) Voxel-wise approach: to evaluate the functional nature of aberrant iFC in preterm born adults (i.e., iFC changes that are independent from underlying GM volume), between group differences in rs-fMRI were tested by entering the GM maps of the VBM analysis as voxel-wise covariates in two-sample *t*-tests, following the biological parametric mapping framework of Casanova et al. (2007). Significance was set at $P < 0.05$ FWE cluster-corrected. 2) ROI-based approach: since we were specifically interested in the quantitative relationship between mutual structural and functional differences, we calculated the spatial overlap of both entities according to the following steps: First, any significant clusters resulting from the ICA analysis were saved as images in SPM8 and subsequently binarized. Exactly the same procedures were performed for the VBM analysis. Second, clusters showing spatial overlap in both entities (as found by visual inspection) were resampled to common space/dimension and multiplied with each other via ImCalc to only spare voxels that showed significant group differences in either domain. Resulting ROIs only contained voxels that showed significant differences in both structural and functional data. Subsequently, ROIs were re-sampled to original space. Only for adults born preterm, ROI-restricted iFC and VBM values were subsequently extracted subject-wise with Matlab-based in-house software and partially correlated with gender, scanner identity, and full-scale IQ as regressors of no interest (partial correlation, $P < 0.05$). We decided to include full-scale IQ as a covariate of no interest into our analysis to be independent of cognitive performance variability, as the primary focus of the present study was on the long-term effects of preterm birth on neurobiological rather than cognitive aspects. As full-scale IQ was not available for 3 subjects, partial correlation is based on the data of 92 subjects. To evaluate whether the structure–function relationship was specific for overlapping aberrant iFC and VBM, we performed analogous partial correlation approaches for group different iFC clusters that were not overlapping with aberrant VBM.

Relationship Between Brain Scores and Measures of Preterm Birth

Exactly the same methodological ROI-based approach as for the relationship between iFC and VBM was used to partially correlate ROI-restricted iFC and VBM values, respectively, with measures of prematurity (GA, BW, and Opti).

Results

Sample Characteristics

One hundred eighty subjects completed MRI examination in Munich ($N = 113$) and Bonn ($N = 67$), respectively. Complete datasets were available for 178 subjects consisting of 83 full-term (52 males) and 95 preterm (54 males) subjects (Table 1). The sample included more males than females ($P = 0.011$), but gender was distributed equally across both groups ($P = 0.43$). Full-term and preterm subjects differed significantly in age at the time of scanning ($P = 0.001$). No differences were found in the SES at birth ($P = 0.88$) or maternal age ($P = 0.97$). By

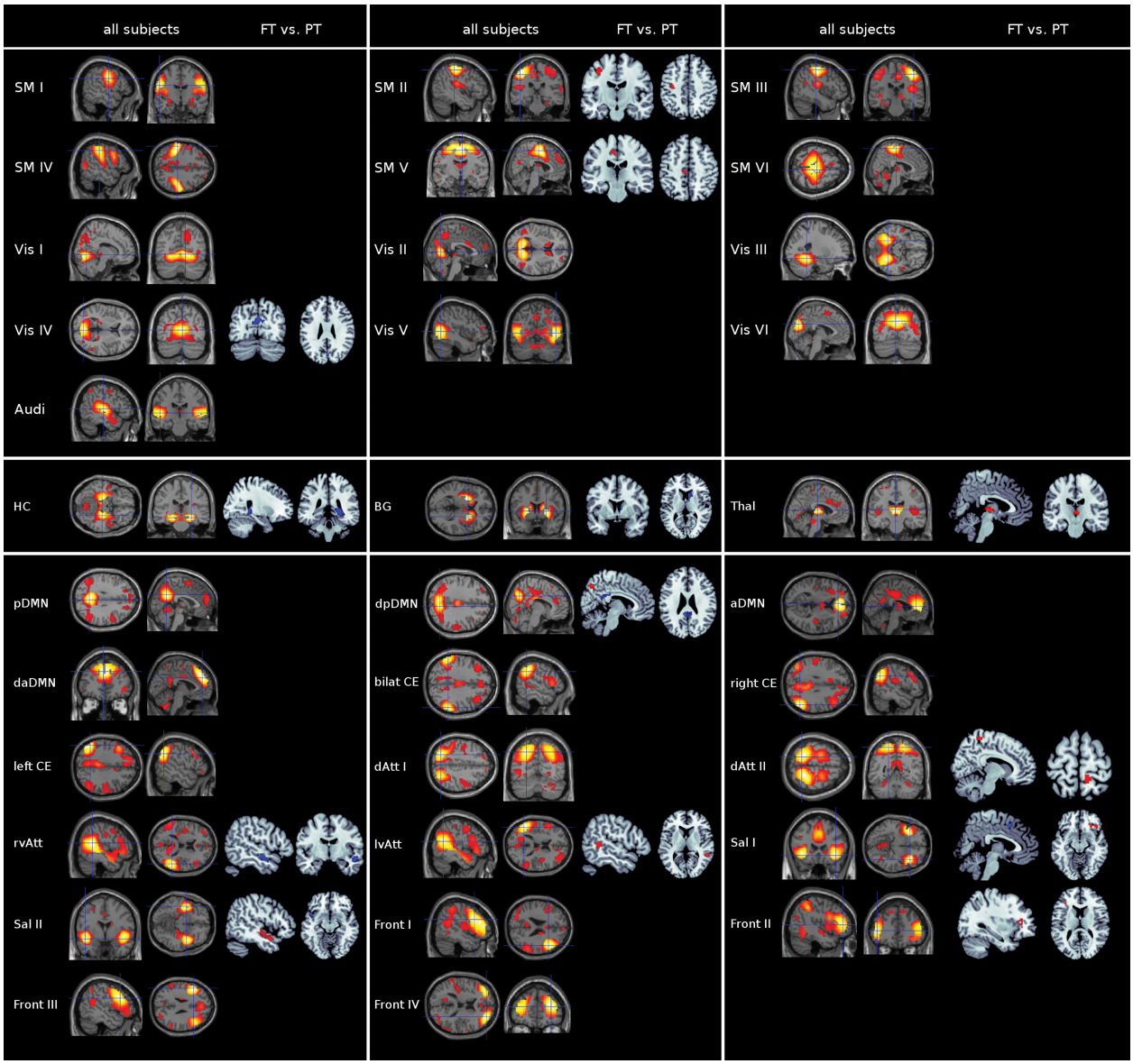

Figure 1. Intrinsic brain networks and correspondent group differences in pre- and full-term born adults at the age of 26 years. Spatial maps are based on all subjects and plotted as *t*-statistical parametric maps (SPM) ($P < 0.05$, FWE-corrected for multiple comparisons, cluster extent >20 voxels). SPMs of full- and preterm (FT, PT) born adults are based on two-sample *t*-tests ($P < 0.05$, FWE cluster-corrected for multiple comparisons; blue: PT < FT; red: PT > FT). Results are arranged according to their classification as unimodal (upper row), subcortical (middle-row), or multimodal networks (bottom row) and displayed at the 2 most informative slices. SM I–VI, sensorimotor networks I–VI; Vis I–VI, visual networks I–VI; Audi, auditory network; HC, hippocampus network; BG, basal ganglia network; Thal, thalamus network; pDMN, posterior default mode network; dpDMN, dorsal posterior default mode network; aDMN, anterior default mode network; daDMN, dorsal anterior default mode network; bilat CE, bilateral central executive network; right CE, right central executive network; left CE, left central executive network; dAtt I, dorsal attention network I; dAtt II, dorsal attention network II; rvAtt, right ventral attention network; lvAtt, left ventral attention network; Sal I, salience network I; Sal II, salience network II; Front I–IV, frontal networks I–IV.

design, adults born preterm had significantly lower GA ($P <$ 0.001), and BW ($P < 0.001$), experienced significantly higher neonatal medical complications (optimality score) ($P < 0.001$) and were hospitalized for longer ($P < 0.001$). Preterm subjects had significantly lower WAIS-III Full-Scale IQ scores ($P =$ 0.001), as well as Verbal IQ ($P = 0.021$) and Performance IQ sub-scores ($P < 0.001$) at age 26 (see Table 1).

Gray-Matter Alterations in Subcortical, Temporal, and Cingulate Areas in Preterm Born Adults

VBM revealed areas of decreased and increased VBM values in preterm adults ($P < 0.05$, FWE-corrected for multiple comparisons; Fig. 2*A*; Supplementary Table 2). Reduced VBM values for GM were found bilaterally in the middle and superior temporal lobes, the caudate, and thalamus. Additionally, there were unilaterally decreased VBM values in the right inferior temporal lobe, the right hippocampus, the right putamen, the right middle occipital lobe, and the left parahippocampus. Preterm born adults also showed some regions with increased VBM values, such as the bilateral anterior and right middle cingulate cortex, the right fusiform area, the right middle orbitofrontal cortex, and the left cerebellum. A full account of the structural alterations in this cohort of preterm born adults will be addressed in a separate publication.

Table 1
Sample characteristics

	Full-term group ($N = 83$)			Preterm group ($N = 95$)			Statistical comparison
	M	SD	Range	M	SD	Range	
Sex (male/female)	52/31			54/41			$P = 0.43$
Age (years)	26.35	±0.43	25.5–27.7	26.59	±0.52	25.7–27.8	$P = 0.001$
GA (weeks)	39.8	±1.03	37–42	30.8	±2.4	25–36	$P < 0.001$
BW (g)	3446	±422	2120–4200	1377	±382	630–2700	$P < 0.001$
Opti (neonatal)	0.36	±0.65	0–3	8.67	±2.59	1–14	$P < 0.001$
Hospital (days)	6.8	±3.1	3–26	70.7	±27.8	19–170	$P < 0.001$
SES	1.94	±0.74	1–3	1.95	±0.76	1–3	$P = 0.88$
Maternal age	29.63	±4.49	16–41	29.66	±5.57	18–42	$P = 0.97$
Full-scale IQ[a]	102	±12	77–130	96	±14	64–132	$P = 0.001$
Verbal IQ[a]	106	±15	77–137	101	±15	62–141	$P = 0.021$
Performance IQ[a]	98	±11	69–123	91	±14	61–118	$P < 0.001$

GA, gestation age; BW, birth weight; Opti (neonatal), optimality score of neonatal conditions, Hospital, duration of hospitalization; SES, socioeconomic status at birth; maternal age, maternal age at birth; Statistical comparisons, sex, SES, χ^2 statistics; age, GA, BW, Hospital, maternal age, IQ, *t*-tests; Opti, nonparametric Mann–Whitney *U*-tests.
[a]Data are based on 92 preterm and 82 full-term subjects, respectively.

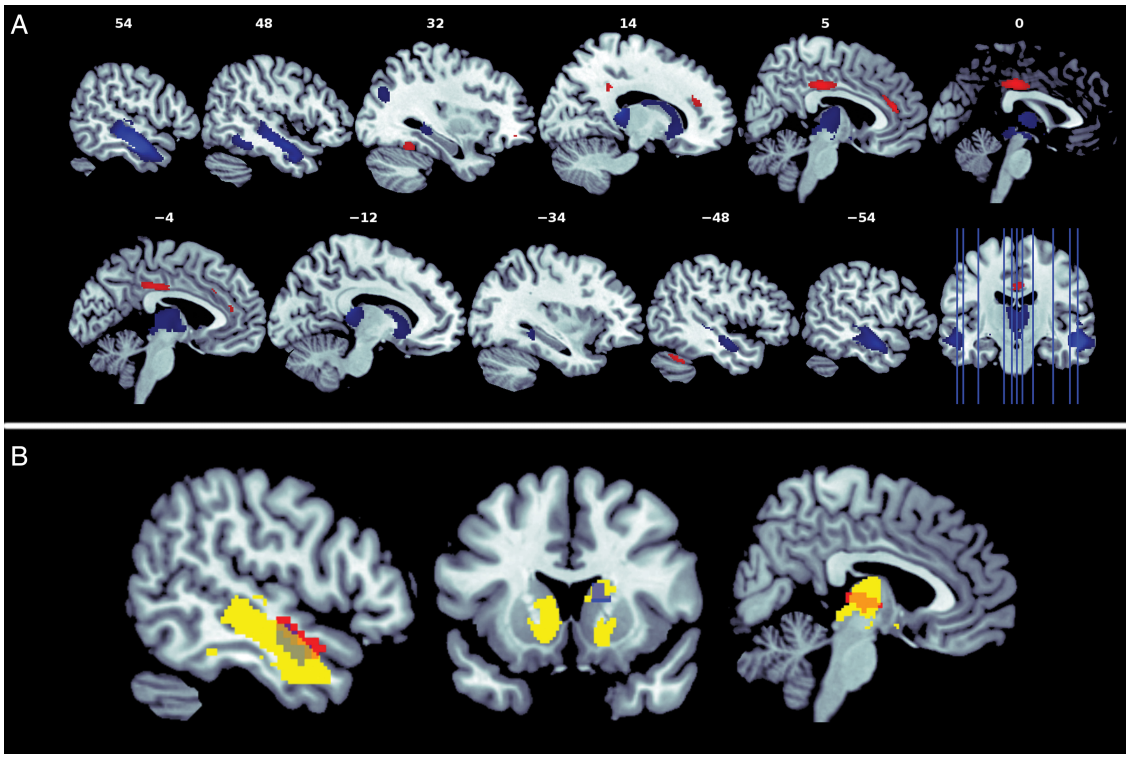

Figure 2. Aberrant gray matter in preterm born adults revealed by voxel-based morphometry overlaps with aberrant intrinsic functional connectivity in the ventral brain. (*A*) Based on structural MRI, differences in VBM were calculated by a two-sample *t*-test thresholded at $P < 0.05$, FWE-corrected for multiple comparisons, cluster extent >20 voxels (blue: PT < FT; red: PT > FT); White numbers on top of each slice represent the *x*-coordinates in MNI space (MNI, Montreal Neurological Institute). (*B*) Overlapping VBM and iFC changes (see Fig. 1). Networks with overlapping iFC and VBM changes are the thalamus network, basal ganglia network, right ventral attention, and salience network II of Figure 1. Aberrant iFC is presented by blue (PT < FT) and red (PT > FT), aberrant VBM by yellow (FT < PT) clusters.

Widespread Alterations of Intrinsic Networks' Connectivity in Preterm Born Adults

ICA revealed unimodal cortical, multimodal cortical and subcortical intrinsic networks for full- and preterm born adults that have been described previously (one-sample *t*-test, $P < 0.05$ FWE-corrected; Fig. 1) (Beckmann et al. 2005; Kiviniemi et al. 2009; Smith et al. 2009; Allen et al. 2011). Unimodal cortical networks included sensory-motor and visual networks, as well as an auditory network. Multimodal cortical networks were composed of networks shown to be involved in cognitive processes such as attention (Fox et al. 2006), salience processing (Seeley et al. 2007), working memory (Imaruoka et al. 2005), executive functioning (Owen et al. 2005), and default mode function (Greicius et al. 2003). Subcortical networks included a basal ganglia network centered on the striatum (Sorg et al. 2013), a network mainly composed of medio-temporal regions centered on the hippocampus (Gour et al. 2011), and one thalamic network (Damoiseaux et al. 2008).

Preterm adults demonstrated widespread differences in the functional connectivity of IBNs across unimodal/multimodal cortical and subcortical networks. In comparison to adults born full-term, we found both decreases and increases in functional connectivity of IBNs ($P < 0.05$; FWE cluster-corrected for multiple comparisons; Fig. 1, Supplementary Table 1).

Unimodal cortical networks: in preterm born adults, increased iFC was found in 2 sensory-motor networks, one lateralized to the left post- and precentral gyrus (SM II; abbreviation refers to that of Fig. 1) and one bilaterally distributed across the supplementary motor area (SM V), while decreased iFC was found in the left cuneus of a visual network along the calcarine fissure. Subcortical networks: altered functional connectivity was found in all 3 subcortical networks. Increased iFC was found in the bilateral thalamus network for left and right thalamus, while decreased iFC was found in the hippocampus network and in the right caudate nucleus of the basal ganglia network. Multimodal cortical networks: consistent with previous findings (Allen et al. 2011), the default mode network was represented by 2 anterior (ventral, dorsal) and 2 posterior (ventral, dorsal) subnetworks. In the dorsal posterior default mode network (dpDMN), preterm adults showed both increased functional connectivity in the right precuneus and decreased functional connectivity in the bilateral posterior cingulate cortex. For attention networks (following Allen's terminology), increased iFC was found in the bilateral dorsal attention network, the left ventral attention network, and in the orbito-insular operculum of the salience network; decreased iFC was found in the right ventral attention network and in the salience network. Finally, increased iFC in the left middle frontal gyrus was found in a frontal network mainly covering the inferior frontal lobe.

To test the functional nature of aberrant iFC in preterm born adults, between group differences in rs-fMRI were subsequently tested by entering the GM maps of the VBM analysis as voxel-wise covariates in two-sample *t*-tests. With the exception of 3 clusters (caudate nucleus of the basal ganglia network; right superior temporal gyrus [STG] of the right ventral attention network; left insula of the salience network), all iFC group differences remained significant ($P < 0.05$ FWE cluster-corrected) (Supplementary Fig. 2), suggesting that most changes in intrinsic connectivity, particularly those in more dorsal brain parts, are independent from structural changes.

Correspondent Changes of Intrinsic Connectivity and Brain Structure Specifically in the Ventral Brain of Preterm Born Adults

In 4 networks, all covering the ventral brain, we found spatial overlap between functional and structural alterations in preterm born adults (Fig. 2*B*). Overlapping regions were located in the right caudate nucleus of the basal ganglia network, in bilateral thalami of the thalamus network, in the right STG of the right ventral attention network, and in the bilateral superior temporal gyri of the salience network II. ROI-based partial correlations between the iFC and VBM values are presented in Figure 3: for the right caudate, which was characterized by decreased VBM values and iFC in the basal ganglia network in

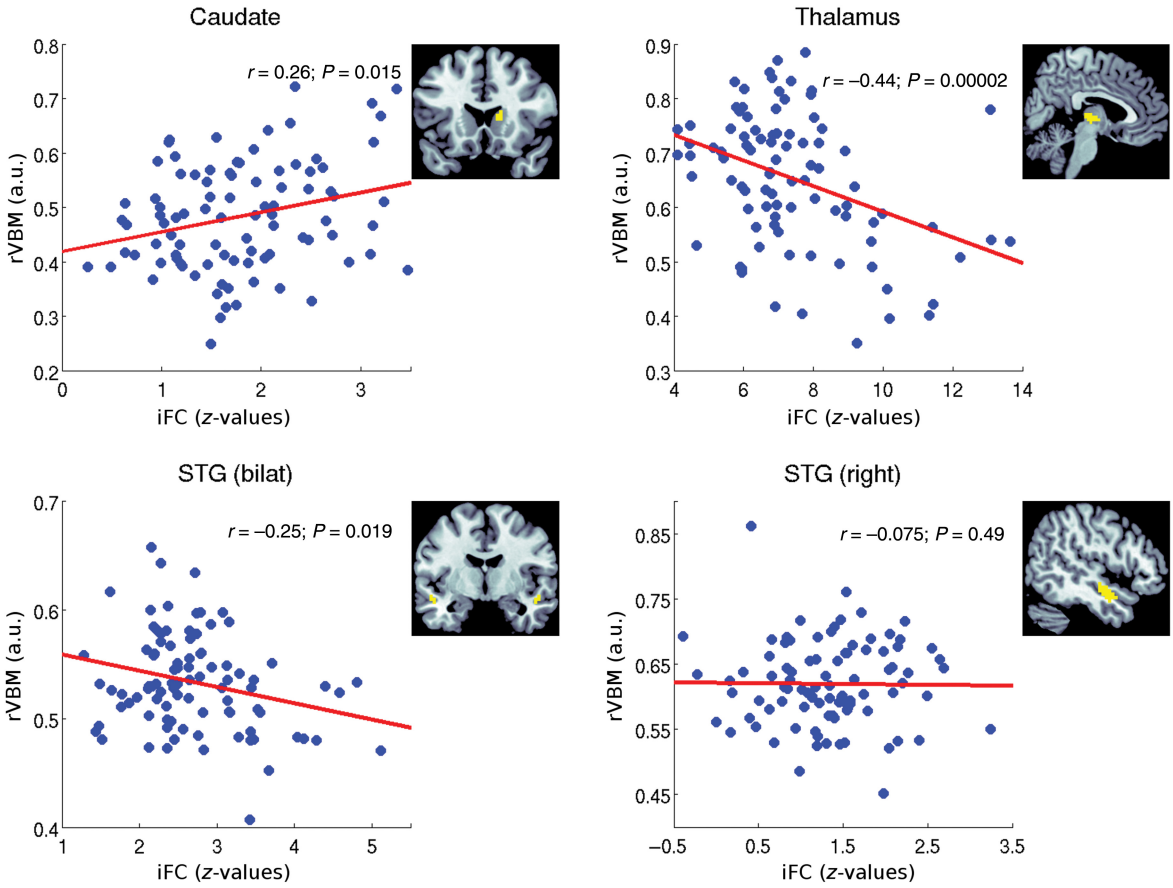

Figure 3. Partial correlations between overlapping aberrant intrinsic functional connectivity (iFC) and regional voxel-based morphometry values (rVBM) in preterm born adults at the age of 26. For 4 intrinsic networks, overlapping aberrant iFC and brain volume was found: in the caudate of the basal ganglia network, in the thalamus of the thalamus network, in the bilateral superior temporal gyrus (bilat. STG) of the salience network II, and in the right STG of the right ventral attention networks (network names are defined in Fig. 1). Partial correlations between overlapping iFC and rVBM are based on data from 92 preterm born adults and included as additional co-variates gender, scanner, and full-scale IQ. iFC is expressed as averaged *z*-values derived from spatial *z*-maps reflecting functional connectivity; rVBM is expressed as averaged regional gray-matter VBM values.

preterm born adults, iFC was positively correlated with VBM values ($r = 0.26$; $P = 0.015$), indicating that higher VBM values were associated with higher functional connectivity. For the thalamus and STG, which both had significantly decreased VBM values and increased iFC in the thalamus and salience network II, respectively, iFC was negatively correlated with VBM values (thalamus $r = -0.44$; $P < 0.0001$; STG $r = -0.25$, $P = 0.019$), indicating that lower VBM values were associated with higher functional connectivity. For the right STG of the right ventral attention network, which was characterized by decreased VBM values and iFC in preterm born adults, iFC and VBM values were not significantly correlated ($r = -0.07$; $P = 0.49$).

To evaluate specificity of correlation between aberrant iFC and VBM in thalamus striatum, and temporal cortex, we performed analogous partial correlation analyses for group different iFC clusters, which were not overlapping with aberrant VBM (see Fig. 1). Only for the hippocampal cluster showing reduced iFC in preterm born adults, we found a significant correlation between iFC and VBM ($r = 0.26$; $P = 0.012$). For all other group different clusters, analyses yielded nonsignificant results. For instance, preterm born adults had significantly increased iFC in the precuneus of the DMN and in the paracentral lobule of the dorsal attention network. However, neither in the precuneus ($r = -0.11$, $P = 0.29$), nor in the paracentral lobule ($r = 0.13$; $P = 0.22$), iFC differences were associated with underlying GM volume. These data indicate inter-related function–structure changes in intrinsic connectivity and brain morphometry specifically in the ventral brain.

Prematurity Measures Predict Correspondent Structural and Functional Changes of the Ventral Brain

Finally, we tested our last hypothesis, namely, that correspondent brain changes in structure and iFC were associated with prematurity measures via partial correlation analysis controlling for gender, scanner identity and full-scale IQ ($P < 0.05$, Fig. 4, Table 2). For thalamus, STG, and caudate, we found significant associations between prematurity measures and VBM or iFC. For example, caudate VBM and iFC values were predicted by the degree of neonatal medical complications (Fig. 4). For details, see Table 2.

Discussion

To investigate the long-term effects of preterm birth on the brain's large-scale intrinsic networks, and their relation to structural brain changes, we performed independent component analysis of resting-state fMRI data and VBM of structural MRI data of 83 full-term and 95 preterm born adults. In preterm born adults, we found widespread alterations of networks' functional connectivity that overlapped and correlated with reduced GM volume specifically in the ventral brain. These results provide first evidence that preterm birth has long-lasting effects on functional connectivity of intrinsic networks, and these changes are specifically related to structural alterations in ventral brain GM. Observed regional specificity supports the view of permanent effects of preterm birth on ventral brain's GM organization into adulthood.

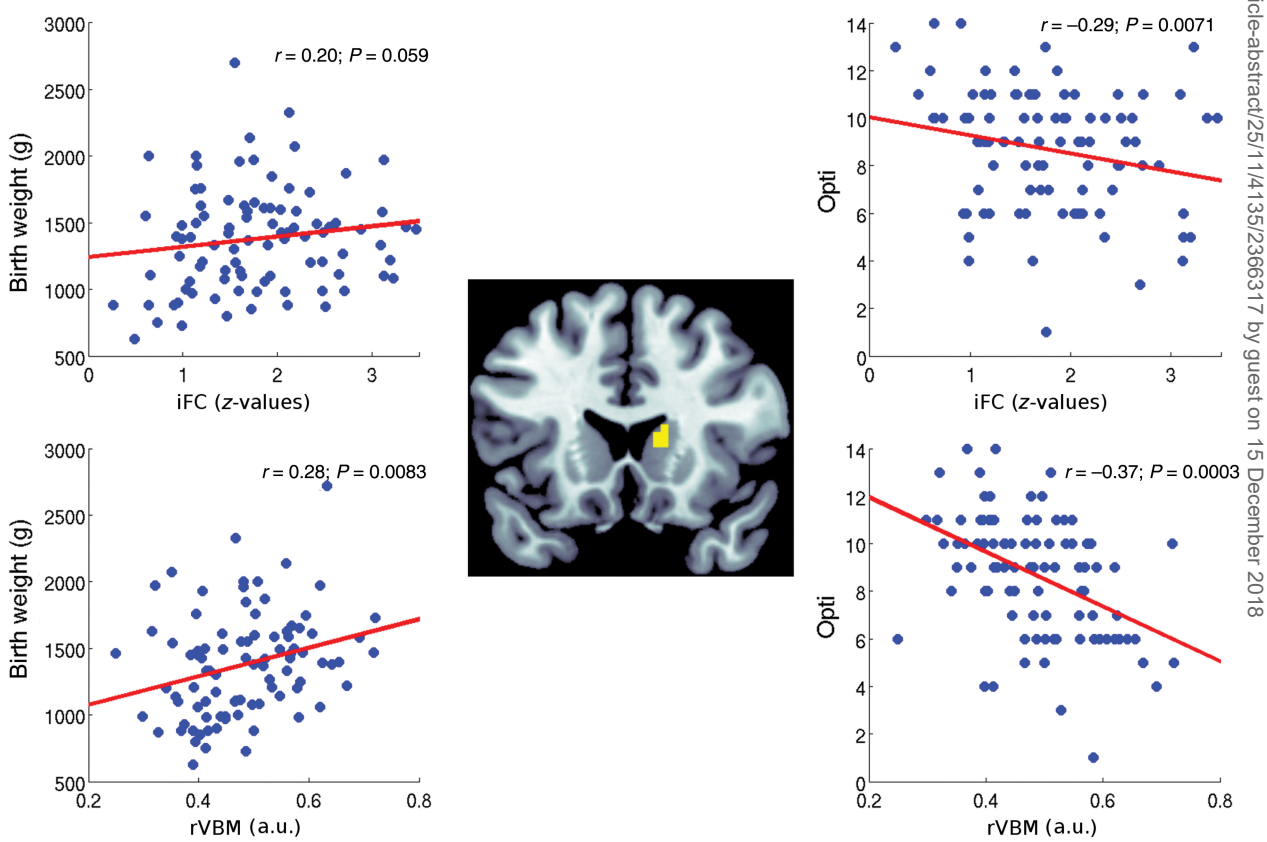

Figure 4. Partial correlations of caudate's intrinsic functional connectivity (iFC) and regional voxel-based morphometry values (rVBM), respectively, with birth weight (BW) and postnatal medical status (Opti). Partial correlations are based on data from 92 preterm born adults and included as additional co-variates gender, scanner, and full-scale IQ. iFC is expressed as averaged *z*-values derived from spatial *z*-maps reflecting functional connectivity; rVBM is expressed as averaged regional gray-matter VBM values.

Table 2
Partial correlation between iFC, rVBM, and parameters of prematurity within overlapping clusters controlling for the effect of gender, scanner ID, and full-scale IQ

Overlapping cluster	iFC/rVBM, *r* (*P*)	Modality	GA, *r* (*P*)	BW, *r* (*P*)	Opti, *r* (*P*)
Thal (bilat)	−0.44 (0.0002)	iFC	–	–	–
		rVBM	0.21 (0.045)	–	−0.24 (0.027)
Caud (right)	0.26 (0.015)	iFC	–	0.20 (0.059)	−0.29 (0.007)
		rVBM	0.34 (0.001)	0.28 (0.008)	−0.37 (0.0003)
STG (bilat)	−0.25 (0.019)	iFC	–	–	–
		rVBM	0.32 (0.002)	0.21 (0.040)	−0.28 (0.007)

iFC, intrinsic functional connectivity; rVBM, regional voxel-based morphometry; GA, gestational age; BW, birth weight; Opti, optimality score of neonatal conditions; bilat, bilateral; Thal, thalamus of the thalamus network; Caud, caudate of the basal ganglia network; STG, superior temporal gyrus of the salience network II; network names are defined in Figure 1.

Aberrant Intrinsic Connectivity and Brain Structure Overlap and Correlate in the Ventral Brain GM of Preterm Born Adults

For preterm born adults, we found overlapping and correlated aberrant intrinsic connectivity and brain structure that was specific for the GM of ventral brain regions such as the caudate, thalamus, and STG (Figs 2 and 3; Table 2). This relationship was found for 3 intrinsic brain networks, that is, the basal ganglia-, thalamus-, and salience network (Table 2). The basal ganglia network was selected by a template-based procedure relying on networks derived from a previous study (Allen et al. 2011), and included mainly striatal regions without cortical involvement (Fig. 1). Thalamus and salience networks were selected by visual inspection and included both noncortical and cortical regions (Fig. 1). All these networks were robustly detected (ICASSO >0.95), covered almost exclusively GM, and correspond well with observed networks of previous studies (Seeley et al. 2007; Kim et al. 2013; Sorg et al. 2013). In the areas of mutual differences, decreased GM volume was associated with both increased (thalamus and STG) and decreased functional connectivity (caudate) in the preterm group (Fig. 3; discussed in detail below). Furthermore, overlapping aberrant iFC or VBM values were predicted by prematurity parameters, suggesting that preterm birth contributes critically to observed altered GM organization (Fig. 4; Table 2). This predictive association was independent of general cognitive abilities, such as IQ, which might be a potential confounder with respect to both preterm birth (Wolke and Meyer 1999) and brain organization (Li et al. 2009).

Correspondently altered ventral GM intrinsic connectivity and structure is in line with previous findings of premature birth. First, animal models of prematurity demonstrated specific and long-lasting effects of perinatal induced hypoxia on both GABA-ergic interneuron maturation and astro-/oligodendrocyte maturation which is essential for regular subcortical white matter development (for review, see Salmaso et al. (2014)). GABA-ergic interneuron maturation and function are critical for synchronized brain activity (Bartos et al. 2007; Huang et al. 2007), while white matter development and function is crucial for structural connectivity. Since both synchronized activity and structural connectivity determine intrinsic network connectivity (Honey et al. 2009), disturbances in these mechanisms may link with currently observed changes in intrinsic connectivity. Second, neuropathological studies in preterm newborns demonstrated that GM changes concentrate on ventral brain areas particularly in the striatum and thalamus, with the more GM changes the more white matter lesions being present (Pierson et al. 2007; Zubiaurre-Elorza et al. 2011). Studies using immunocytochemical approaches revealed specifically impaired white matter axons, subplate neurons that guide thalamo-cortical neuronal development, and late migrating neurons (Robinson et al. 2006; Haynes et al. 2008; Andiman et al. 2010; Kinney et al. 2012). In line with these neuropathological studies, in-vivo imaging in preterm born newborns found specifically altered GM mainly in thalamus and basal ganglia (Inder et al. 2005; Srinivasan et al. 2007; Ball et al. 2012). Particularly thalamus volume reductions covary with GM volumes of the striatum, insular, frontal, and temporal cortex, which together constitute a brain pattern similar to the atrophy pattern found in preterm born adolescences and adults (see also current results of Fig. 2) (Ball et al. 2012). Together with related white matter reductions (Pierson et al. 2007; Srinivasan et al. 2007; Ball et al. 2012), these data suggest substantial and lasting impact of preterm birth on the thalamo-cortical system including basal ganglia. Our current results of correspondently changed intrinsic connectivity and brain structure add to these findings in a regionally and mechanistically consistent way: after preterm birth, changes in ventral brain GM structure of newborns seem to last into adulthood (Fig. 2), they link with aberrant functional connectivity of affected intrinsic networks (Fig. 3), and they are specific for striatum, thalamus, and ventral cortex (Figs 1 and 2). Given impaired GABA-ergic interneuron development and compromised astro-/oligodendrocyte-based white matter maturation as seen in animal models of perinatal induced hypoxia, our data suggest such initial lesions to lead to long-lasting GM reorganization in preterm born individuals, which is characterized by correspondingly altered GM structure and intrinsic connectivity.

With respect to this model, 2 further aspects of our findings should be mentioned. First, the observed correspondence between aberrant intrinsic connectivity and brain structure was specific for the ventral brain. While we found several iFC changes in more dorsal brain networks such as in the attention or default mode network, we found no relation of these changes with regional VBM scores in preterm born subjects. This finding suggests that altered dorsal brain intrinsic connectivity links with underlying GM structure in a distinct way than ventral brain connectivity changes. One might speculate whether this difference reflects distinct types of relationship between destructive and maturational/adaptive processes with stronger destructive impact of preterm birth on ventral brain areas (Volpe 2009). This model implicates dorsal networks to be more involved in compensatory processes. Future studies are necessary to test these suggestions. Second, we found a complex relationship between reduced GM volume and altered iFC. While in the basal ganglia network, caudate atrophy was positively linked with reduced iFC, in thalamus and salience

network, thalamus and STG atrophy was negatively linked with increased iFC in preterm born adults. We suggest that several factors might contribute to this complex relationship: 1) the pattern of connectivity, that is, while the basal ganglia network is mainly restricted to intrastriatal connectivity, the other 2 networks include thalamo-cortical or cortico-cortical connectivity; 2) while the striatum is dominated by GABA-ergic inhibitory neurons, thalamus and cortex include both glutamate-ergic excitatory and GABA-ergic inhibitory neurons; 3) microstructure of striatum, thalamus, and cortex are strongly different from each other. Future studies are needed to better understand how these different factors might impact altered GM intrinsic connectivity–brain structure relationship after preterm delivery.

Preterm Born Adults Show Widespread Differences in the iFC of Intrinsic Brain Networks

To the best of our knowledge, this is the first study that investigates the whole ensemble of intrinsic brain networks in preterm born adults (Fig. 1). We identified networks that were highly consistent with previous findings in healthy controls (Kiviniemi et al. 2009; Smith et al. 2009; Allen et al. 2011; Kim et al. 2013), suggesting the reliability of our analysis approach. Most aberrant iFC clusters particularly those in the dorsal brain of preterm born adults remained significant after controlling for structural changes (see Supplementary Fig 2), demonstrating the functional nature of iFC changes. Differences in network connectivity were characterized by both increased and decreased iFC in unimodal cortical, multimodal cortical and subcortical networks (see Fig. 1). A detailed discussion of single iFC differences between preterm and term born adults particularly with respect to previous findings (Gozzo et al. 2009; Myers et al. 2010; Smyser et al. 2010; Wilke et al. 2013; White et al. 2014) and its potential functional significance is given in the supplement.

Methodological Issues and Limitations

The detailed discussion of methodological issues and limitations such as sample bias, the use of ICA to detect intrinsic networks, white matter injuries, and applied prematurity scores is given in the supplement.

Conclusion

The current study provides first evidence for correspondent aberrant GM intrinsic connectivity and brain structure in preterm born adults specifically in the ventral brain. Results suggest particular and lasting ventral brain GM re-organization after preterm delivery.

Supplementary Material

Supplementary material can be found at: http://www.cercor.oxfordjournals.org/.

Funding

This study was supported by German Federal Ministry of Education and Science (BMBF 01ER0801 to N.B. and D.W., BMBF 01EV0710 to A.M.W., BMBF 01ER0803 to C.S.) and the Kommission für Klinische Forschung, Technische Universität München (KKF 8765162 to C.S.). We are grateful to the staff of the Department of Neuroradiology in Munich and the Department of Radiology in Bonn for their help in data collection.

Notes

We thank all current and former members of the Bavarian Longitudinal Study Group who contributed to general study organization, recruitment, and data collection, management and subsequent analyses, including (in alphabetical order): Stephan Czeschka, Claudia Grünzinger, Christian Koch, Diana Kurze, Sonja Perk, Andrea Schreier, Antje Strasser, Julia Trummer, and Eva van Rossum. Most importantly, we thank all our study participants for their efforts to take part in this study. *Conflict of Interest*: None declared *Financial Disclosures*: All authors report no biomedical financial interests or potential conflicts of interest.

References

Allen EA, Erhardt EB, Damaraju E, Gruner W, Segall JM, Silva RF, Havlicek M, Rachakonda S, Fries J, Kalyanam R et al. 2011. A baseline for the multivariate comparison of resting-state networks. Front Syst Neurosci. 5:2.

Andiman SE, Haynes RL, Trachtenberg FL, Billiards SS, Folkerth RD, Volpe JJ, Kinney HC. 2010. The cerebral cortex overlying periventricular leukomalacia: analysis of pyramidal neurons. Brain Pathol. 20:803–814.

Ashburner J, Friston KJ. 2005. Unified segmentation. Neuroimage. 26:839–851.

Ashburner J, Friston KJ. 2000. Voxel-based morphometry—the methods. Neuroimage. 11:805–821.

Ball G, Boardman JP, Rueckert D, Aljabar P, Arichi T, Merchant N, Gousias IS, Edwards AD, Counsell SJ. 2012. The effect of preterm birth on thalamic and cortical development. Cereb Cortex. 22:1016–1024.

Bartos M, Vida I, Jonas P. 2007. Synaptic mechanisms of synchronized gamma oscillations in inhibitory interneuron networks. Nat Rev Neurosci. 8:45–56.

Bauer A. 1988. Ein Verfahren zur Messung des für das Bildungsverhalten relevanten Sozial Status (BRSS)—überarbeitete Fassng. Frankfurt, Germany: Deutsches Institut für Internationale Pädagogische Forschung.

Beckmann CF, DeLuca M, Devlin JT, Smith SM. 2005. Investigations into resting-state connectivity using independent component analysis. Philos Trans R Soc Lond B Biol Sci. 360:1001–1013.

Biswal B, Yetkin FZ, Haughton VM, Hyde JS. 1995. Functional connectivity in the motor cortex of resting human brain using echo-planar MRI. Magn Reson Med. 34:537–541.

Bressler SL, Menon V. 2010. Large-scale brain networks in cognition: emerging methods and principles. Trends Cogn Sci. 14:277–290.

Casanova R, Srikanth R, Baer A, Laurienti PJ, Burdette JH, Hayasaka S, Flowers L, Wood F, Maldjian JA. 2007. Biological parametric mapping: a statistical toolbox for multimodality brain image analysis. Neuroimage. 34:137–143.

Damaraju E, Phillips JR, Lowe JR, Ohls R, Calhoun VD, Caprihan A. 2010. Resting-state functional connectivity differences in premature children. Front Syst Neurosci. 4. doi:10.3389/fnsys.2010.00023.

Damoiseaux JS, Beckmann CF, Arigita EJ, Barkhof F, Scheltens P, Stam CJ, Smith SM, Rombouts SA. 2008. Reduced resting-state brain activity in the "default network" in normal aging. Cereb Cortex. 18:1856–1864.

Damoiseaux JS, Rombouts SA, Barkhof F, Scheltens P, Stam CJ, Smith SM, Beckmann CF. 2006. Consistent resting-state networks across healthy subjects. Proc Natl Acad Sci USA. 103:13848–13853.

Deng W. 2010. Neurobiology of injury to the developing brain. Nat Rev Neurol. 6:328–336.

Doria V, Beckmann CF, Arichi T, Merchant N, Groppo M, Turkheimer FE, Counsell SJ, Murgasova M, Aljabar P, Nunes RG et al. 2010. Emergence of resting state networks in the preterm human brain. Proc Natl Acad Sci USA. 107:20015–20020.

Dubowitz LM, Dubowitz V, Goldberg C. 1970. Clinical assessment of gestational age in the newborn infant. J Pediatr. 77:1–10.
Eikenes L, Lohaugen GC, Brubakk AM, Skranes J, Haberg AK. 2011. Young adults born preterm with very low birth weight demonstrate widespread white matter alterations on brain DTI. Neuroimage. 54:1774–1785.
Erhardt EB, Rachakonda S, Bedrick EJ, Allen EA, Adali T, Calhoun VD. 2011. Comparison of multi-subject ICA methods for analysis of fMRI data. Hum Brain Mapp. 32:2075–2095.
Fox MD, Corbetta M, Snyder AZ, Vincent JL, Raichle ME. 2006. Spontaneous neuronal activity distinguishes human dorsal and ventral attention systems. Proc Natl Acad Sci USA. 103:10046–10051.
Fox MD, Raichle ME. 2007. Spontaneous fluctuations in brain activity observed with functional magnetic resonance imaging. Nat Rev Neurosci. 8:700–711.
Fransson P, Skiold B, Engstrom M, Hallberg B, Mosskin M, Aden U, Lagercrantz H, Blennow M. 2009. Spontaneous brain activity in the newborn brain during natural sleep--an fMRI study in infants born at full term. Pediatr Res. 66:301–305.
Fransson P, Skiold B, Horsch S, Nordell A, Blennow M, Lagercrantz H, Aden U. 2007. Resting-state networks in the infant brain. Proc Natl Acad Sci USA. 104:15531–15536.
Gour N, Ranjeva JP, Ceccaldi M, Confort-Gouny S, Barbeau E, Soulier E, Guye M, Didic M, Felician O. 2011. Basal functional connectivity within the anterior temporal network is associated with performance on declarative memory tasks. Neuroimage. 58:687–697.
Gozzo Y, Vohr B, Lacadie C, Hampson M, Katz KH, Maller-Kesselman J, Schneider KC, Peterson BS, Rajeevan N, Makuch RW et al. 2009. Alterations in neural connectivity in preterm children at school age. Neuroimage. 48:458–463.
Greicius MD, Krasnow B, Reiss AL, Menon V. 2003. Functional connectivity in the resting brain: a network analysis of the default mode hypothesis. Proc Natl Acad Sci USA. 100:253–258.
Griffiths ST, Gundersen H, Neto E, Elgen I, Markestad T, Aukland SM, Hugdahl K. 2013. fMRI: blood oxygen level-dependent activation during a working memory-selective attention task in children born extremely preterm. Pediatr Res. 74:196–205.
Gutbrod T, Wolke D, Soehne B, Ohrt B, Riegel K. 2000. Effects of gestation and birth weight on the growth and development of very low birthweight small for gestational age infants: a matched group comparison. Arch Dis Child Fetal Neonatal Ed. 82:208–214.
Haynes RL, Billiards SS, Borenstein NS, Volpe JJ, Kinney HC. 2008. Diffuse axonal injury in periventricular leukomalacia as determined by apoptotic marker fractin. Pediatr Res. 63:656–661.
Honey CJ, Sporns O, Cammoun L, Gigandet X, Thiran JP, Meuli R, Hagmann P. 2009. Predicting human resting-state functional connectivity from structural connectivity. Proc Natl Acad Sci USA. 106:2035–2040.
Horovitz SG, Fukunaga M, de Zwart JA, van Gelderen P, Fulton SC, Balkin TJ, Duyn JH. 2008. Low frequency BOLD fluctuations during resting wakefulness and light sleep: a simultaneous EEG-fMRI study. Hum Brain Mapp. 29:671–682.
Huang ZJ, Di Cristo G, Ango F. 2007. Development of GABA innervation in the cerebral and cerebellar cortices. Nat Rev Neurosci. 8:673–686.
Imaruoka T, Saiki J, Miyauchi S. 2005. Maintaining coherence of dynamic objects requires coordination of neural systems extended from anterior frontal to posterior parietal brain cortices. Neuroimage. 26:277–284.
Inder TE, Warfield SK, Wang H, Huppi PS, Volpe JJ. 2005. Abnormal cerebral structure is present at term in premature infants. Pediatrics. 115:286–294.
Kim DJ, Park B, Park HJ. 2013. Functional connectivity-based identification of subdivisions of the basal ganglia and thalamus using multilevel independent component analysis of resting state fMRI. Hum Brain Mapp. 34:1371–1385.
Kinney HC, Haynes RL, Xu G, Andiman SE, Folkerth RD, Sleeper LA, Volpe JJ. 2012. Neuron deficit in the white matter and subplate in periventricular leukomalacia. Ann Neurol. 71:397–406.
Kiviniemi V, Starck T, Remes J, Long X, Nikkinen J, Haapea M, Veijola J, Moilanen I, Isohanni M, Zang YF et al. 2009. Functional segmentation of the brain cortex using high model order group PICA. Hum Brain Mapp. 30:3865–3886.
Li Y, Liu Y, Li J, Qin W, Li K, Yu C, Jiang T. 2009. Brain anatomical network and intelligence. PLoS Comput Biol. 5:e1000395.
Meng C, Brandl F, Tahmasian M, Shao J, Manoliu A, Scherr M, Schwerthoffer D, Bauml J, Forstl H, Zimmer C et al. 2013. Aberrant topology of striatum's connectivity is associated with the number of episodes in depression. Brain. 137:598–609.
Mullen KM, Vohr BR, Katz KH, Schneider KC, Lacadie C, Hampson M, Makuch RW, Reiss AL, Constable RT, Ment LR. 2011. Preterm birth results in alterations in neural connectivity at age 16 years. Neuroimage. 54:2563–2570.
Murphy K, Bodurka J, Bandettini PA. 2007. How long to scan? The relationship between fMRI temporal signal to noise ratio and necessary scan duration. Neuroimage. 34:565–574.
Myers EH, Hampson M, Vohr B, Lacadie C, Frost SJ, Pugh KR, Katz KH, Schneider KC, Makuch RW, Constable RT et al. 2010. Functional connectivity to a right hemisphere language center in prematurely born adolescents. Neuroimage. 51:1445–1452.
Nosarti C, Giouroukou E, Healy E, Rifkin L, Walshe M, Reichenberg A, Chitnis X, Williams SC, Murray RM. 2008. Grey and white matter distribution in very preterm adolescents mediates neurodevelopmental outcome. Brain. 131:205–217.
Nosarti C, Shergill SS, Allin MP, Walshe M, Rifkin L, Murray RM, McGuire PK. 2009. Neural substrates of letter fluency processing in young adults who were born very preterm: alterations in frontal and striatal regions. Neuroimage. 47:1904–1913.
Owen AM, McMillan KM, Laird AR, Bullmore E. 2005. N-back working memory paradigm: a meta-analysis of normative functional neuroimaging studies. Hum Brain Mapp. 25:46–59.
Pierson CR, Folkerth RD, Billiards SS, Trachtenberg FL, Drinkwater ME, Volpe JJ, Kinney HC. 2007. Gray matter injury associated with periventricular leukomalacia in the premature infant. Acta Neuropathol. 114:619–631.
Prechtl HF. 1967. Neurological sequelae of prenatal and perinatal complications. Br Med J. 4:763–767.
Riegel K, Orth B, Wolke D, Osterlund K. 1995. Die Entwicklung gefährdet geborener Kinder bis zum 5 Lebensjahr. Stuttgart, Germany: Thieme.
Robinson S, Li Q, Dechant A, Cohen ML. 2006. Neonatal loss of gamma-aminobutyric acid pathway expression after human perinatal brain injury. J Neurosurg. 104:396–408.
Salmaso N, Jablonska B, Scafidi J, Vaccarino FM, Gallo V. 2014. Neurobiology of premature brain injury. Nat Neurosci. 17:341–346.
Seeley WW, Menon V, Schatzberg AF, Keller J, Glover GH, Kenna H, Reiss AL, Greicius MD. 2007. Dissociable intrinsic connectivity networks for salience processing and executive control. J Neurosci. 27:2349–2356.
Selip DB, Jantzie LL, Chang M, Jackson MC, Fitzgerald EC, Boll G, Murphy A, Jensen FE. 2012. Regional differences in susceptibility to hypoxic-ischemic injury in the preterm brain: exploring the spectrum from white matter loss to selective grey matter injury in a rat model. Neurol Res Int. 2012:725184.
Sepulcre J, Liu H, Talukdar T, Martincorena I, Yeo BT, Buckner RL. 2010. The organization of local and distant functional connectivity in the human brain. PLoS Comput Biol. 6:e1000808.
Smith SM, Fox PT, Miller KL, Glahn DC, Fox PM, Mackay CE, Filippini N, Watkins KE, Toro R, Laird AR et al. 2009. Correspondence of the brain's functional architecture during activation and rest. Proc Natl Acad Sci USA. 106:13040–13045.
Smyser CD, Inder TE, Shimony JS, Hill JE, Degnan AJ, Snyder AZ, Neil JJ. 2010. Longitudinal analysis of neural network development in preterm infants. Cereb Cortex. 20:2852–2862.
Sorg C, Riedl V, Muhlau M, Calhoun VD, Eichele T, Laer L, Drzezga A, Forstl H, Kurz A, Zimmer C et al. 2007. Selective changes of resting-state networks in individuals at risk for Alzheimer's disease. Proc Natl Acad Sci USA. 104:18760–18765.
Sorg C, Manoliu A, Neufang S, Myers N, Peters H, Schwerthoffer D, Scherr M, Muhlau M, Zimmer C, Drzezga A et al. 2013. Increased intrinsic brain activity in the striatum reflects symptom dimensions in schizophrenia. Schizophr Bull. 39:387–395.

Spencer MD, Moorhead TW, Gibson RJ, McIntosh AM, Sussmann JE, Owens DG, Lawrie SM, Johnstone EC. 2008. Low birthweight and preterm birth in young people with special educational needs: a magnetic resonance imaging analysis. BMC Med. 6:1.

Srinivasan L, Dutta R, Counsell SJ, Allsop JM, Boardman JP, Rutherford MA, Edwards AD. 2007. Quantification of deep gray matter in preterm infants at term-equivalent age using manual volumetry of 3-tesla magnetic resonance images. Pediatrics. 119:759–765.

Van Dijk KR, Sabuncu MR, Buckner RL. 2012. The influence of head motion on intrinsic functional connectivity MRI. Neuroimage. 59:431–438.

Vincent JL, Patel GH, Fox MD, Snyder AZ, Baker JT, Van Essen DC, Zempel JM, Snyder LH, Corbetta M, Raichle ME. 2007. Intrinsic functional architecture in the anaesthetized monkey brain. Nature. 447:83–86.

Volpe JJ. 2009. Brain injury in premature infants: a complex amalgam of destructive and developmental disturbances. Lancet Neurol. 8:110–124.

Von Aster M, Neubauer A, Horn R. 2006. Wechsler Intelligenztest für Erwachsene (WIE). Deutschsprachige Bearbeitung und Adaptation des WAIS-III von David Wechsler. Frankfurt/Main, Germany: Harcourt Test Services.

White TP, Symington I, Castellanos NP, Brittain PJ, Froudist Walsh S, Nam KW, Sato JR, Allin MP, Shergill SS, Murray RM et al. 2014. Dysconnectivity of neurocognitive networks at rest in very-preterm born adults. Neuroimage Clin. 4:352–365.

Wilke M, Hauser TK, Krageloh-Mann I, Lidzba K. 2013. Specific impairment of functional connectivity between language regions in former early preterms. Hum Brain Mapp. doi:10.1002/hbm.22408.

Wolke D, Meyer R. 1999. Cognitive status, language attainment, and prereading skills of 6-year-old very preterm children and their peers: the Bavarian Longitudinal Study. Dev Med Child Neurol. 41:94–109.

Zubiaurre-Elorza L, Soria-Pastor S, Junque C, Segarra D, Bargallo N, Mayolas N, Romano-Berindoague C, Macaya A. 2011. Gray matter volume decrements in preterm children with periventricular leukomalacia. Pediatr Res. 69:554–560.